Available online at www.sciencedirect.com
ScienceDirect
Ceramics International 36 (2010) 1609–1614
CERAMICS INTERNATIONAL
www.elsevier.com/locate/ceramint

Thermal conductivity in mullite/ZrO_2 composite coatings

E. García, J. Mesquita-Guimarães, M.I. Osendi, P. Miranzo *

Instituto de Cerámica y Vidrio, CSIC, Kelsen 5, 28049 Madrid, Spain

Received 28 December 2009; received in revised form 16 January 2010; accepted 18 February 2010
Available online 25 March 2010

Abstract

Mullite-based multilayered structures have been suggested as promising environmental barrier coatings for Si_3N_4 and SiC ceramics. Mullite has been used as bottom layer because its thermal expansion coefficient closely matches those of the Si-based substrates, whereas Y–ZrO_2 has been tried as top layer due to its stability in combustion environments. In addition, mullite/ZrO_2 compositions may work as middle layers to reduce the thermal expansion coefficient mismatch between the ZrO_2 and mullite layers. Present work studies the thermal behaviour of a flame sprayed mullite/ZrO_2 (75/25, v/v) composite coating. The changes in crystallinity, microstructure and thermal conductivity of free-standing coatings heat treated at two different temperatures (1000 and 1300 °C) are comparatively discussed. The as-sprayed and 1000 °C treated coatings showed an almost constant thermal conductivity (K) of 1.5 W m^{-1} K^{-1}. The K of the 1300 °C treated specimen increased up to twice due to the extensive mullite crystallization without any cracking.

Keywords: C. Thermal conductivity; D. ZrO_2; D. Mullite; Environmental barrier coatings

1. Introduction

The development of the new generation of turbines and microturbines for higher working temperatures requires the use of ceramic components based on Si_3N_4 and SiC. Under dry oxidative environments, these materials present excellent high temperature oxidation resistance due to the growth of the protective silica layer but, under the stringent working conditions of temperature and steam of gas turbine engines, they experience water vapour corrosion leading to a surface recession through the destruction of the SiO_2 layer and, consequently, to dimensional changes in the ceramic component [1–3]. To overcome this problem, the so-called environmental barrier coatings (EBC) have been designed. However, reliable coatings are still far away due to the multiple requirements that need to be considered, being one of them the significant properties mismatch with substrate materials and, therefore, new prospects are being directed to accommodate these mismatches by the designing of multilayered/graded systems [4,5].

One of the earliest protective layers intended was mullite [6] due to its close thermal expansion coefficient to Si_3N_4. However, formation of cracks due to re-crystallization after high temperature exposure and some SiO_2 layer recession were reported [7]. Several attempts in mullite containing multilayered systems have been tried with different degree of success, looking for corrosion protection and limiting residual thermal stresses. A single 7 wt.% Y_2O_3 doped ZrO_2 (YSZ) topcoat on mullite was the first choice but recently coatings based on BSAS (BaO–SrO–Al_2O_3–SiO_2)/mullite, rare earth silicates/mullite [8–11] and $La_2Hf_2O_7$/mullite [12] structures are at the cutting edge. Among the rare earth silicates, monosilicates (RE_2SiO_5; RE = rare earth element) as Yb_2SiO_5 [13,14] and disilicates like $Lu_2Si_2O_7$ [15,16], which show good phase stability and thermal expansion coefficient close to silicon-based ceramic substrates, have been tried. In general, these EBCs experience lower volatility and higher chemical compatibility under combustion environments than BSAS coatings, reducing the crack density as well. A monolayer system of $ZrSiO_4$ has also been probed as top-coat having low porosity and good adhesion to the substrate [17]. Recently, Zr/Hf-mixed silicates have been evaluated as potential EBCs [18].

In addition to the studies on new materials and structures for EBCs systems, current works are involved in analysing their

* Corresponding author. Tel.: +34 917355872; fax: +34 917355843.
E-mail address: pmiranzo@icv.csic.es (P. Miranzo).

0272-8842/$36.00
doi:10.1016/j.ceramint.2010.02.037

behaviour under real working conditions, i.e. combustion gases and high temperatures. Actually, the recession behaviour [7,14,19], the water vapour corrosion resistance [15,16], the impact resistance [20], the residual stresses built-up [21] and the thermal cycling response [22,23] have been studied in these layered coatings. Their degradation by melts produced in combustion environments [24] and the evaluation of non-destructive techniques to monitor the coatings degradation [25] have been additional topics of interest.

In progress works on mullite coatings for EBC applications are focused on increasing their crystallinity and mechanical properties [26]. One well-known way to improve the mechanical performance of mullite is the addition of tetragonal ZrO_2 particles, which enhances at the same time hardness and toughness. Monoclinic ZrO_2 powders can be used since the tetragonal polymorph of ZrO_2 is retained at room temperature due to the constraint imposed by the surrounding matrix [27]. Mullite/ZrO_2 coatings could work as intermediate layer in multilayered EBCs, reducing the thermal expansion coefficient mismatch between the YSZ top-coat and the mullite bond coat. In a previous work of the present authors, mullite/ZrO_2 coatings were flame sprayed on both ceramic and metal substrates [28] and their crystallinity was promoted by heating at temperatures in the range of 1000–1300 °C, with an associated increase in hardness and elastic modulus. In fact, crack-free crystalline coatings having good mechanical properties were readily produced by in situ annealing the coatings with the oxyacetylene torch. To the best of our knowledge, there is little work devoted to study the thermal conductivity (K) of mullite-based coatings [29] despite the fact that it is one of the key properties that determines the performance of EBCs. The aim of this paper is to study the influence of the amorphous/crystalline nature of free-standing mullite/ZrO_2 flame sprayed coatings on the thermal conductivity. As-sprayed coatings were mostly amorphous and their crystallization was enhanced by heat treating them at temperatures in the range of 1000–1300 °C. The effect of crystallization on the thermal conductivity is deeply discussed.

2. Experimental procedure

Commercial mullite ($3Al_2O_3{\cdot}2SiO_2$) (Baikolox SASM. Baikowski Chimie, France) and monoclinic ZrO_2 (SF-EXTRA, Z-Tech Zirconia, USA) powders were the starting materials. Particle size distributions were measured by laser diffraction (Mastersizer S, Malvern, UK) methods. The mean particle size (d_{50}) for mullite was 1.53 μm, with a distribution width between 0.05 and 80 μm. The ZrO_2 particle size spanned from 0.05 to 40 μm, with d_{50} of 1.21 μm. Mullite/ZrO_2 agglomerates with composition 75/25 (v/v), showing good flowability through the feeding system, were prepared in the same way as described elsewhere [30]. Briefly, a mullite/ZrO_2 water suspension with 30 wt.% of solid content, plus 0.4 wt.% of a polyelectrolyte dispersant and 5 wt.% of a polysaccharide binder, was thoroughly blended. Afterwards, the slurry was spray dried with a rotary atomizer spray dryer (Mobile Minor Spray Dryer, basic model, Niro Atomizer, Denmark) in a co-current flow. The spray dried (SD) mullite/ZrO_2 batch showed a quasi mono-modal particle size distribution, with d_{50} at 23 μm (Fig. 1).

Free-standing specimens were produced by flame spraying powders over smooth ($R_z < 20$ μm) metallic substrates (2.5 cm × 2.5 cm × 0.3 cm), using an oxygen–acetylene flame spraying gun (model CastoDyn DS 8000, Eutectic Castolin, Spain). The spraying conditions were: acetylene/oxygen volumetric flow ratio of 1.1, gas pressures of 7×10^4 Pa (C_4H_4) and 4×10^5 Pa (O_2), input power of 28 kW, stand-off distance of 20 cm and a powder feed rate of ∼1.2 kg h^{-1}. Coatings of 600–800 μm in thickness were built up with a programmed transverse scan speed of 0.7 m s^{-1}, a scanning step of 1 cm, and 4 consecutive passes. Substrate temperature remained below 800 °C, checked by a K-type thermocouple in contact with one of the substrate edges. The coatings crystallinity was promoted by furnace heating free-standing specimens at 1000 and 1300 °C for 12 h, using heating and cooling rates of 5 °C min^{-1}.

The microstructure of the different coatings was analyzed using a field emission scanning electron microscope (FEM, Hitachi S-4700, Japan) provided with energy-dispersive X-ray spectroscopy (EDS) analysis. Crystalline phases in the coatings were identified by X-ray diffraction analysis (XRD–Siemens D5000, Germany).

A corresponding bulk composite was processed for comparison. In this case, mullite and ZrO_2 mixtures were ball milled for 21 h in isopropyl alcohol using nylon balls as milling media. Alcohol media was eliminated in a rotary-evaporator to avoid phase segregation. Then, the powder mixture was dried at 65 °C, sieved through a 100 μm mesh, uniaxially pressed at 45 MPa and furnace treated at 1600 °C for 1 h.

The thermal diffusivity (α) of coatings and bulk sample was measured by the laser-flash method (Thermaflash 2200, Holometrix, USA) in Ar atmosphere, as a function of temperature, from 25 to 800 °C. Disks of 12.7 mm in diameter were drilled from the free-standing coatings and ground to get flat specimens. Bulk material was machined in a similar way. Prior to thermal diffusivity measurements, both the front and the back faces of each specimen were coated with a thin gold

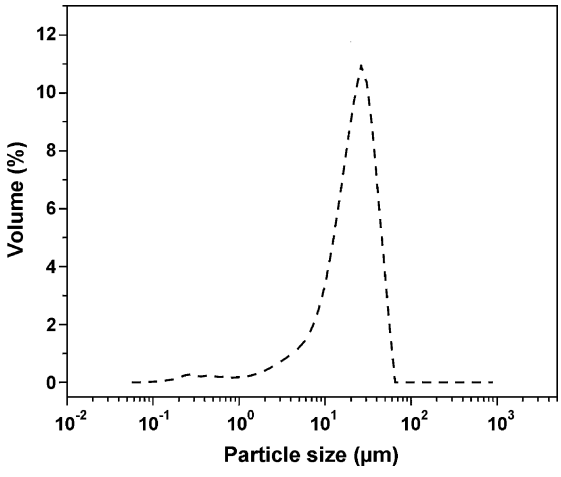

Fig. 1. Particle size distribution of the spray dried powders.

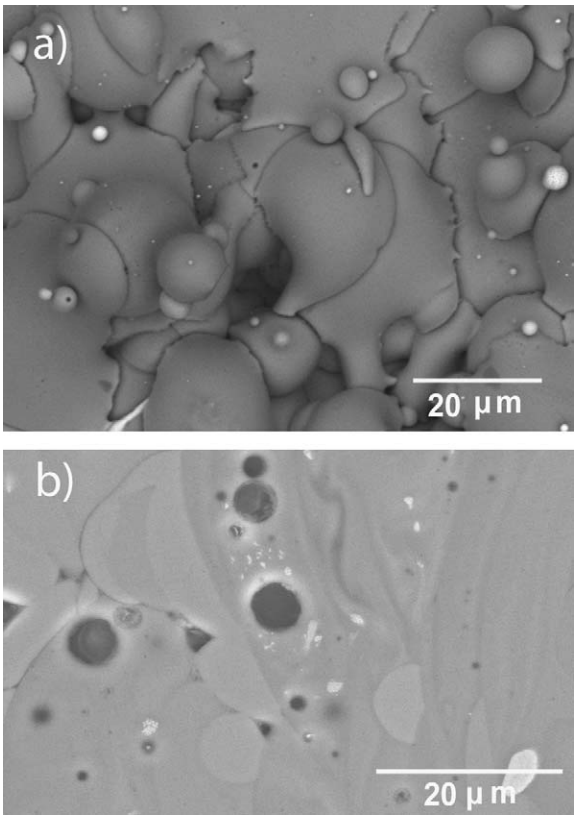

Fig. 2. SEM micrographs of as-sprayed coating: (a) top view and (b) polished cross-section.

layer, followed by deposition of a thin carbon layer, in order to enhance heat absorption at the surface and to prevent direct transmission of the laser beam. The specific heat (C_p) as a function of temperature was calculated from the chemical composition and the heat capacity data of the constituent oxides (ZrO_2 and mullite) obtained from literature sources [31]. Thermal conductivity (K) was then obtained from α, C_p and the mass density (ρ) measured by water immersion, using the following expression:

$$K = \alpha \rho C_p \quad (1)$$

3. Results and discussion

Coatings top view (Fig. 2a) shows mostly melted disk-shaped splats of about 20–30 μm, in accordance with the size of the powder feedstock. In the polished cross-section (Fig. 2b), splats of different colour that correspond to local variations in composition are seen. As discussed in a previous paper [28], most of the splats have compositions along the mullite–ZrO_2 tie-line, but few have less SiO_2 content than the original powders, due to local volatilizations during the flame spraying process. Splats look smooth but some small crystals are occasionally observed (Fig. 2b).

The XRD pattern of the as-sprayed coating (Fig. 3) shows a broad band at 30° (2θ) with overlaid weak peaks, which correspond to mullite, m-ZrO_2 (m = monoclinic) and t-ZrO_2 (t = tetragonal). On the other hand, the 1000 °C treated coating shows strong peaks of t-ZrO_2 and traces of mullite and m-ZrO_2 (Fig. 3). The broadening of the peaks indicates the nucleation of crystallites with very small size, 10 nm for t-ZrO_2 and 18 nm for mullite crystals, as estimated by the Scherrer's expression [32]. These values may be slightly underestimated as the instrumental broadening correction was not considered. At 1300 °C, both t-ZrO_2 and mullite peaks become narrower and more intense, indicating the practical full crystallization of the amorphous phases. Grain growth was evidenced in the 1000 and 1300 °C coatings by SEM observations; as an example, Fig. 4 shows the extensive crystallization of ZrO_2 for the 1300 °C coating. In a previous work [33] of present authors, the crystallinity ratio (C.R.) was defined as the ratio between the area under the peaks and the area under the whole XRD pattern, normalized to the fully crystallized 1300 °C coating. The C.R. is 0.26 for the 1000 °C coating, close to the weight fraction of

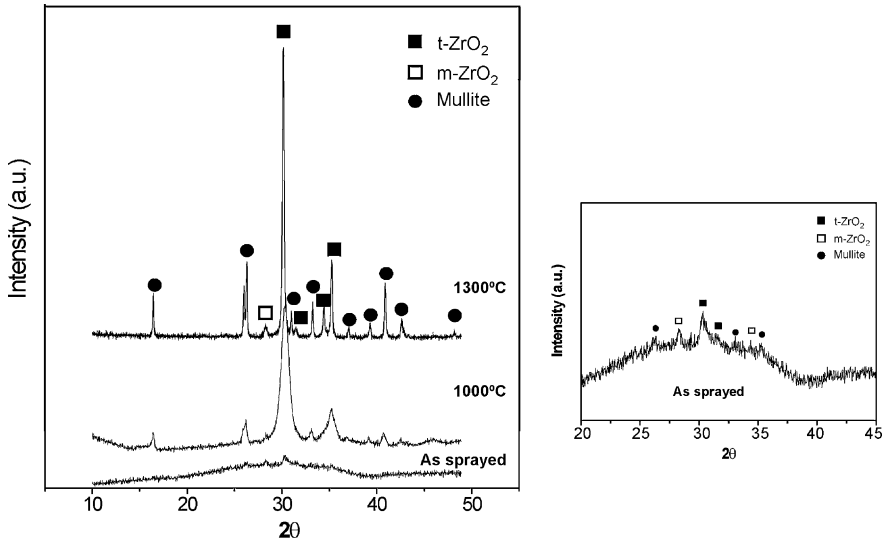

Fig. 3. XRD patterns of as-sprayed and heat treated mullite/ZrO_2 coatings. An enlarged view of the as-sprayed coating pattern is also depicted.

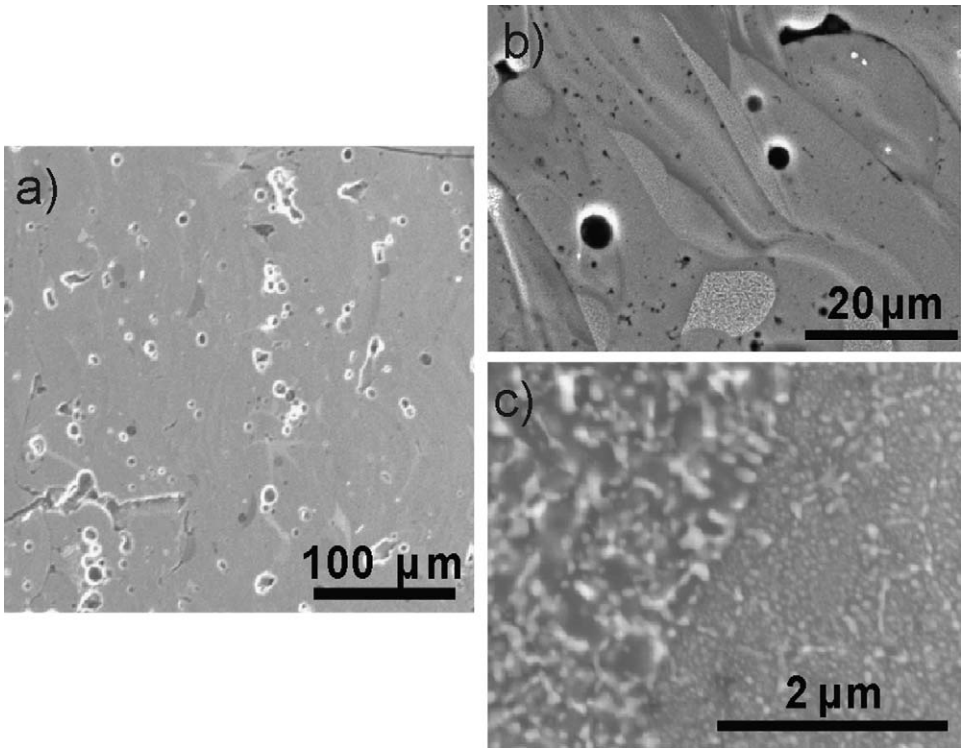

Fig. 4. SEM micrographs at three different magnifications of the polished cross-section of the coating treated at 1300 °C.

ZrO_2 (0.39), pointing that for this treatment mainly ZrO_2 nucleates.

Moreover, cracking is not detected after crystallization (Fig. 4a) but instead the formation of very small spherical pores is observed (Fig. 4b). The porosity in the coatings (17–13%) reduces the elastic moduli (126–177 GPa [28]), which probably contributes to inhibit crack formation during crystallization. The appearance of small spherical pores in the heated coatings is explained by the lower mass density of the mullite/ZrO_2 composition in the amorphous state. In fact, porous-free solid amorphous mullite/ZrO_2 beads, obtained by flame spraying (FS) the feedstock in water, have a mass density of 3600 kg m^{-3}, which is lower than the value of 3800 kg m^{-3} obtained for the SD feedstock powder before flame spraying, both measured by helium pycnometry. The value for the SD powders is very close to the theoretical mass density (3840 kg m^{-3}) calculated from the rule of mixtures, considering the given volume fractions and theoretical densities of mullite (3160 kg m^{-3}) and m-ZrO_2 (5900 kg m^{-3}). Despite the formation of microporosity, the open and total porosities of the coatings (Table 1) slightly decrease after heating, which infers that some sintering has occurred. Total porosity has been calculated considering the mass density of the FS beads as the theoretical mass density of the as-sprayed amorphous coating; whereas, for the crystalline coatings, the theoretical mass density of reference was that of the SD crystalline powders. For the 1000 °C treated coating, the theoretical mass density was calculated using the rule of mixtures, the relative amount of amorphous and crystalline phases estimated from XRD patterns and the corresponding densities.

Thermal diffusivity as a function of temperature for as-sprayed and heat treated mullite/ZrO_2 free-standing coatings are depicted in Fig. 5a. As seen in the plots, thermal diffusivity does not show any significant change for the 1000 °C treated coating, despite the incipient crystallization observed by XRD (Fig. 3), but it strongly increases for the 1300 °C treated specimen. In consonance, thermal conductivity shows similar trend (Fig. 5b), increasing from 1.4 W m^{-1} K^{-1} at room temperature for the as-sprayed and 1000 °C coatings up to 2.7 W m^{-1} K^{-1} for the fully crystallized 1300 °C coating. The values are almost constant in the whole temperature range and similar to those reported for YSZ -TBCs, which vary between 1 and 2.2 W m^{-1} K^{-1} depending on the coating technique, i.e. plasma spray or electron beam physical vapour deposition [34,35]. Therefore, these amorphous mullite/ZrO_2 coatings would be effective thermal barriers with very low thermal conductivity up to temperatures of 1000 °C.

Table 1
Mass density, open and total porosity of the mullite/ZrO_2 coatings.

Specimen	Mass density[a] (kg m^{-3})	Open porosity[a] (%)	Porosity[b] (%)
As-sprayed	3000	10.0	17
1000 for 12 h	3100	9.5	14
1300 for 12 h	3300	6.4	13

[a] Measured by water immersion.
[b] Calculated assuming that theoretical densities of the as-sprayed and heat treated coatings are those measured by helium pycnometry for the FS beads and SD powders, respectively.

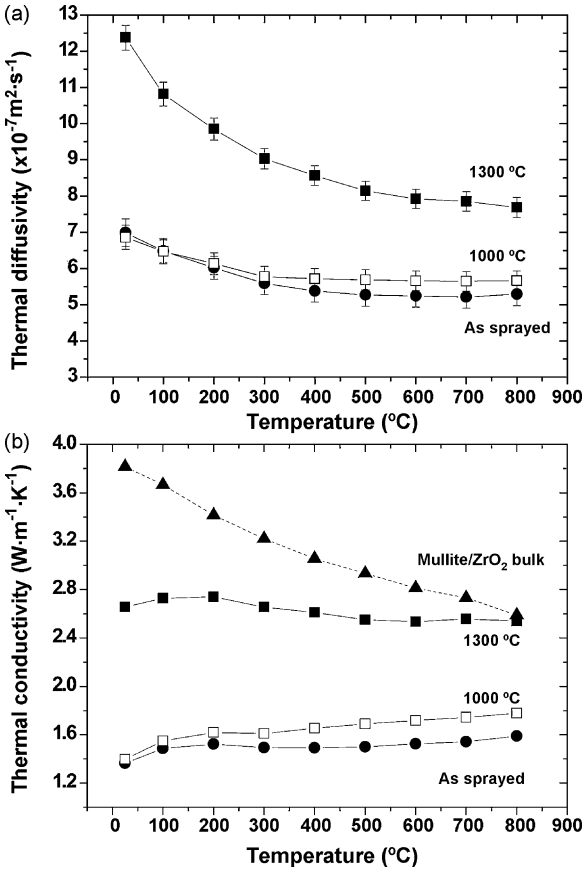

Fig. 5. Thermal diffusivity (a) and thermal conductivity (b) as a function of temperature for as-sprayed and heat treated mullite/ZrO_2 free-standing coatings. Values of thermal conductivity of a mullite/ZrO_2 bulk material are plotted for comparison.

The thermal conductivity measured in the mullite/ZrO_2 bulk specimen with 15% of porosity, plotted in Fig. 5b as well, gave a value of 3.8 W m^{-1} K^{-1} at room temperature that is much higher than the data measured for any of these composite coatings. The temperature dependence of thermal conductivity for the mullite/ZrO_2 composite can be fitted to a $T^{-0.3}$ function, similarly to the behaviour reported for bulk mullite [36], which is consistent with a phonon–phonon scattering mechanism in the high temperature regimen. Conversely, the lower K value measured at room temperature for the amorphous as-sprayed coating is typical of a glass-like material, whose thermal conductivity is characterized by a diffusive vibrational wave-packet [37]. Similar behaviour is observed for the coating treated at 1000 °C, as this coating still has a significant amount of amorphous phase (crystallinity ratio of 0.26). Considering the concept of minimum thermal conductivity [37,38], we can asses that K_{min} for the amorphous mullite/ZrO_2 coating is ~1.4 W m^{-1} K^{-1}, which is slightly lower than values measured for dense highly disordered YSZ and fused SiO_2 (2 W m^{-1} K^{-1}), probably due to the porosity content (17%) of that coating.

Certainly, the thermal conductivity of these coatings depends on both the amount of amorphous phase and the porosity content. The 4% reduction in porosity after the 1300 °C treatment would lead to a 7% increase in its thermal conductivity, according to Klemens' equation [39]. Therefore, porosity reduction itself does not explain the significant increase in K (95%), which can only be attributed to the crystallization of amorphous phases. The thermal conductivity of the 1300 °C treated coating is almost constant with temperature and still 20% lower than thermal conductivity of the mullite/ZrO_2 bulk composite at room temperature. As the mullite/ZrO_2 composite has similar porosity to the coating, this difference must be linked to either the very small size of the crystallizations, about 100 nm (Fig. 4c), or the particular orientation of the inter-splat porosity in the coatings, perpendicular to the heat flow, as usually occurs in thermal sprayed coatings [40].

4. Conclusions

The presence of amorphous phases is decisive for the thermal conductivity of flame sprayed coatings, reducing in 50% the thermal conductivity of similar but crystalline coating. For present mullite/ZrO_2 coatings (75/25, v/v), values as low as 1.4 W m^{-1} K^{-1}, almost constant with temperature, are obtained for amorphous coatings. The limit working temperature for these amorphous coatings, while taking advantage of its low K, would be 1000 °C.

Acknowledgements

This work has been supported by MICINN (Spain) under Grant No. MAT2006-07118 and by CSIC under NRC (Canada)–CSIC (Spain) Joint Project. Eugenio Garcia acknowledges the "Ramón y Cajal Program" of the MICINN for his financial support.

References

[1] J.L. Smialek, R.C. Robinson, E.J. Opila, D.S. Fox, N.S. Jacobson, SiC and Si_3N_4 recession due to SiO_2 scale volatility under combustor conditions, Adv. Compos. Mater.: Off. J. Jpn. Soc. Compos. Mater. 8 (1) (1999) 33–45.
[2] K.L. More, P.F. Tortorelli, M.K. Ferber, J.R. Keiser, Observations of accelerated silicon carbide recession by oxidation at high water-vapour pressures, J. Am. Ceram. Soc. 83 (1) (2000) 211–213.
[3] R.C. Robinson, J.L. Smialek, SiC recession caused by SiO_2 scale volatility under combustion conditions: I. Experimental results and empirical model, J. Am. Ceram. Soc. 82 (7) (1999) 1817–1825.
[4] M. Belmonte, Advanced ceramic materials for high temperature applications, Adv. Eng. Mater. 8 (8) (2006) 693–703.
[5] P.D. Sarkisov, N.V. Popovich, L.A. Orlova, Y.E. Ennaneva, Barrier coatings for type C/SiC ceramic–matrix composites (Review), Glass Ceram. 65 (9–10) (2008) 366–371.
[6] K.N. Lee, R.A. Miller, N.S. Jacobson, New generation of plasma-sprayed mullite coatings on silicon carbide, J. Am. Ceram. Soc. 78 (3) (1995) 705–710.
[7] S. Ueno, T. Ohji, H.T. Lin, Corrosion and recession of mullite in water vapour environment, J. Eur. Ceram. Soc. 28 (2008) 431–435.
[8] K.N. Lee, J.I. Eldridge, R.C. Robinson, Residual stresses and their effects on the durability of environmental barrier coatings for SiC ceramics, J. Am. Ceram. Soc. 88 (12) (2005) 3483–3488.
[9] K.L. More, P.F. Tortorelli, L.R. Walker, J.B. Kimmel, N. Miriyala, J.R. Price, H.E. Eaton, E.Y. Sun, G.D. Linsey, Evaluating Environmental

Barrier Coatings on Ceramic Matrix Composites after Engine and Laboratory Exposures, American Society of Mechanical Engineers, International Gas Turbine Institute, Turbo Expo (Publication) IGTI, Amsterdam, 2002
[10] I. Spitsberg, J. Steibel, Thermal and environmental barrier coatings for SiC/SiC CMCs in aircraft engine applications, Int. J. Appl. Ceram. Technol. 1 (4) (2004) 291–301.
[11] K.N. Lee, D.S. Fox, J.I. Eldridge, D. Zhu, R.C. Robinson, N.P. Bansal, R.A. Miller, Upper temperature limit of environmental barrier coatings based on mullite and BSAS, J. Am. Ceram. Soc. 86 (8) (2003) 1299–1306.
[12] S. Latzel, R. Vassen, D. Stöver, New environmental barrier coating system on carbon-fibre reinforced silicon carbide composites, J. Therm. Spray Technol. 14 (2) (2005) 268–272.
[13] K.N. Lee, D.S. Fox, N.P. Bansal, Rare earth silicate environmental barrier coatings for SiC/SiC composites and Si_3N_4 ceramics, J. Eur. Ceram. Soc. 25 (2005) 1705–1715.
[14] S. Ueno, T. Ohji, H.T. Lin, Recession behaviour of $Yb_2Si_2O_7$ phase under high speed steam jet at high temperatures, Corros. Sci. 50 (2008) 178–182.
[15] S. Ueno, D.D. Jayaseelan, T. Ohji, Development of oxide-based EBC for silicon nitride, Int. J. Appl. Ceram. Technol. 1 (2004) 362–373.
[16] S. Ueno, H.T. Lin, T. Ohji, Corrosion and recession mechanism of $Lu_2Si_2O_7$/mullite eutectic, J. Eur. Ceram. Soc. 28 (2008) 2359–2361.
[17] M. Suzuki, S. Sodeoka, T. Inoue, Zircon-based ceramics composite coating for environmental barrier coating, J. Therm. Spray Technol. 17 (3) (2008) 404–409.
[18] K. Nakano, N. Fokatsu, Y. Kanno, Thermodynamics of Zr/Hf-mixed silicates as a potential for environmental barrier coatings for Tyrannohex materials, Surf. Coat. Technol. 203 (2009) 1997–2002.
[19] S. Ueno, T. Ohji, H.T. Lin, Recession behaviour of a silicon nitride with multi-layered environmental barrier coating system, Ceram. Int. 33 (2007) 859–862.
[20] R.T. Bhatt, S.R. Choi, L.M. Cosgriff, D.S. Fox, K.N. Lee, Impact resistance of environmental barrier coated SiC/SiC composites, Mater. Sci. Eng. A 456 (2008) 8–19.
[21] B.J. Harder, J.D. Almer, C.M. Weyant, K.N. Lee, K.T. Faber, Residual stress analysis of multilayer environmental barrier coatings, J. Am. Ceram. Soc. 92 (2) (2009) 452–459.
[22] K. Kokini, Y.R. Takeuchi, B.D. Choules, Surface thermal cracking of thermal barrier coatings owing to stress relaxation: zirconia vs. mullite, Surf. Coat. Technol. 82 (1–2) (1996) 77–82.
[23] A. Gilbert, K. Kokini, S. Sankarasubramanian, Thermal fracture of zirconia–mullite composite thermal barrier coatings under thermal shock: a numerical study, Surf. Coat. Technol. 102 (2008) 2152–2161.
[24] K.M. Grant, S. Krämer, J.P.A. Löfvander, C.G. Levi, CMAS degradation of environmental barrier coatings, Surf. Coat. Technol. 202 (2007) 653–657.
[25] M.D. Chambers, P.A. Rousseve, D.R. Clarke, Luminescence thermometry for environmental barrier coating materials, Surf. Coat. Technol. 203 (2008) 461–465.
[26] E. Garcia, J. Mesquita-Guimarães, P. Miranzo, M.I. Osendi, C.V. Cojocaru, Y. Wang, C. Moreau, R.S. Lima, Phase composition and microstructural responses of crystalline mullite/YSZ coating under water vapour environments, Proc. International Thermal Spray Conference and Exposition (ITSC 2010), in press.
[27] J.S. Moya, M.I. Osendi, Microstructure and mechanical properties of mullite/ZrO_2 composites, J. Mater. Sci. 19 (9) (1984) 2909–2914.
[28] C. Cano, E. Garcia, A.L. Fernandes, M.I. Osendi, P. Miranzo, Mullite/ZrO_2 coatings produced by flame spraying, J. Eur. Ceram. Soc. 28 (11) (2008) 2191–2197.
[29] U. Steinhauser, W. Braue, J. Gőring, B. Kanka, H. Schneider, A new concept for thermal protection of all-mullite composites in combustion chambers, J. Eur. Ceram. Soc. 20 (2000) 651–658.
[30] E. Garcia, J. Guimarães, P. Miranzo, M.I. Osendi, Y. Wang, R.S. Lima, C. Moreau, Mullite and mullite/ZrO_2-7 wt% Y_2O_3 powders for thermal spraying of environmental barrier coatings, J. Therm. Spray Technol. 19 (1–2) (2010) 286–293.
[31] M.W. Chase, *NIST-JANAF* Thermochemical Tables, 4th ed., J. Phys. Chem. Ref. Data Monograph 9, Parts I & II, ACS & AIP, Woodbury, 1998.
[32] H.P. Klug, L.E. Alexander, X-ray Diffraction Procedures for Polycrystalline and Amorphous Materials, 2nd ed., John Wiley & Sons, New York, NY, 1974.
[33] J. Mesquita-Guimarães, E. Garcia, P. Miranzo, M.I. Osendi, Crystallization studies in mullite and mullite-YSZ beads, J. Eur. Ceram. Soc., in press.
[34] C.G. Levi, Emerging materials and processes for thermal barrier systems, Curr. Opin. Solid State Mater. Sci. 8 (1) (2004) 77–91.
[35] U. Schulz, U.C. Leyens, K. Fritscher, M. Peters, B. Saruhan-Brings, O. Lavigne, J.M. Dorvaux, M. Poulain, R. Mévrel, M. Caliez, Some recent trends in research and technology of advanced thermal barrier coatings, Aerospace Sci. Technol. 7 (1) (2003) 73–80.
[36] R. Barea, M.I. Osendi, J.M.F. Ferreira, P. Miranzo, Thermal conductivity of highly porous mullite material, Acta Mater. 53 (2005) 3313–3318.
[37] D.G. Cahill, S.K. Watson, R.O. Pohl, Lower limit to the thermal conductivity of disordered crystals, Phys. Rev. B 46 (10) (1992) 6131–6140.
[38] D.R. Clarke, S.R. Phillpot, Thermal barrier coating materials, Mater. Today 8 (6) (2005) 22–29.
[39] P.G. Klemens, Thermal conductivity of inhomogeneous media, High Temp.–High Press. 23 (1991) 241–248.
[40] E. Garcia, P. Miranzo, R. Soltani, T.W. Coyle, Microstructure and thermal behaviour of thermal barrier coatings, J. Therm. Spray Technol. 17 (4) (2008) 478–485.